ELSEVIER

Journal of Power Sources 73 (1998) 229–241

JOURNAL OF POWER SOURCES

Modeling fuel cell stack systems

J.H. Lee [a,*], T.R. Lalk [b]

[a] *Los Alamos National Laboratory, Los Alamos, NM 87545, USA*
[b] *Dept. of Mech. Eng., Texas A&M University, College Station, TX 77843-3123, USA*

Received 26 September 1997; accepted 5 December 1997

Abstract

A technique for modeling fuel cell stacks is presented along with the results from an investigation designed to test the validity of the technique. The technique was specifically designed so that models developed using it can be used to determine the fundamental thermal–physical behavior of a fuel cell stack for any operating and design configuration. Such models would be useful tools for investigating fuel cell power system parameters. The modeling technique can be applied to any type of fuel cell stack for which performance data is available for a laboratory scale single cell. Use of the technique is demonstrated by generating sample results for a model of a Proton Exchange Membrane Fuel Cell (PEMFC) stack consisting of 125 cells each with an active area of 150 cm^2. A PEMFC stack was also used in the verification investigation. This stack consisted of four cells, each with an active area of 50 cm^2. Results from the verification investigation indicate that models developed using the technique are capable of accurately predicting fuel cell stack performance.

Keywords: Fuel cells; Electrochemistry; Mathematical modeling; Design

1. Introduction

A fuel cell is an electrochemical device that combines hydrogen and oxygen, with the aid of electrocatalysts, to produce electricity. A single fuel cell has a potential of about 0.7 V when generating a current of approximately 500 mA/cm^2. Such cells are arranged in stacks to produce a useful voltage (100 to 300 V). For terrestrial applications, the oxygen for the reaction is supplied from atmospheric air and the hydrogen can be produced from many sources, including natural gas, coal, biomass, and solar energy used to electrolyze water.

A fuel cell has several advantages over currently existing energy conversion devices. These include the type and amount of emissions they produce and their efficiency. A fuel cell produces only electricity, water, and heat, thereby eliminating pollution at the energy conversion device. In contrast, existing energy conversion devices are responsible for a majority of the emissions that degrade the air quality of most cities. The first law efficiency of fuel cells can reach as high as 50%. This is higher than every type of energy conversion devices commonly used today.

Many parameters are associated with fuel cell power systems; parameters are anything that affects the design or performance of the system. An abbreviated list of the parameters of a fuel cell power system is shown in Table 1. The list is separated into operating and design parameters. Operating parameters deal with the fuel cell system operating conditions whereas the design parameters are those associated with the system configuration.

To understand the relative importance of the parameters and parameter interactions an investigation of the parameters is needed. An investigative technique that is well suited for this task is mathematical modeling. This is because a model can be developed that is easily changed; allowing different configurations of a system to be simulated. This reduces the time and cost associated with a parameter investigation [1].

A technique for modeling fuel cell power systems was developed that will aid in designing models to be used for investigating system parameters. Models developed using this technique have a modular design and simulate non-steady state operating conditions while making only minimal steady state assumptions. The modular design makes a model easy to modify which is necessary when investigating alternative combinations of system design and operat-

* Corresponding author.

0378-7753/98/$19.00

Table 1
Important parameters for a fuel cell vehicle power system

Parameter	Description
Operating	
· Pressure	Fuel and air operating pressures of the fuel cell stack.
· Temperature	Target point for the stack operating temperature.
· Humidity	The relative humidity of the air entering the stack.
· Stoichiometry	The amount of excess fuel and air that is delivered to the stack. May be different for fuel and air.
Design	
Membrane–electrode assembly	
· Membrane	Type and thickness of material.
· Catalyst	Type and amount used on each electrode.
· Electrode	Material for electrode and amount and type of impregnation material
Stack	
· MEA active area	Active area of the membrane–electrode assemblies (MEA).
· Aspect ratio	Ratio of the bipolar plates length to width.
· Number of cells	Number of fuel cells in a stack.
· Plate material	Construction material of the bipolar plates.
· Flow configuration	Relationship of fuel entry point to the air entry point.
· Gas delivery strategy	Means of getting the gasses through the stack.
· Cooling plate material	Construction material of the cooling plates.
· Cooling fluid	Fluid used to cool the stack.
· Cooling plate frequency	Number of fuel cells between cooling plates.
· Stack construction	Means of connecting the individual components.

ing parameters, and when advances in technology result in the performance of system components changing. The technique incorporates nonsteady state simulation to enable investigation of transients associated with startup, shut down, and changing load. This increases accuracy when investigating applications that have highly dynamic operating conditions, such as automobiles.

The remainder of this paper briefly describes a fuel cell stack and explains the modeling technique used to develop fuel cell stack models. In addition, the technique was applied to a Proton Exchange Membrane Fuel Cell (PEMFC) stack and sample output from the resulting model is given. Finally, the results of a verification investigation are presented.

2. Description of a fuel cell stack

A diagram of a typical section of a fuel cell stack is shown in Fig. 1. The individual cells, referred to as Membrane–Electrode Assemblies (MEA), are composed of a membrane (electrolyte) sandwiched between two porous electrodes. The MEAs produce direct current electricity. Bipolar plates, which are electrically conducting, separate the MEAs as well as provide a means for delivery of the fuel and oxidant to the reaction sites located at the electrode/membrane interface. The basic unit is repeated to build up a stack. A complete multi-cell stack may include cooling plates, which are specially designed bipolar plates. These plates are designed to control stack temperature.

The main factors that determine the maximum amount of electricity that can be produced by a fuel cell stack are the number of cells (MEAs) and the active area (surface area producing electricity) of the cells. The voltage of a stack is determined by the number of cells it contains and the current is determined by the active area of the cells. Each cell contributes approximately 1 V to the total voltage of the stack while the larger the area, the greater the maximum current.

The modeling technique described in this paper was developed using the electrochemical equations and experimental volt–ampere characteristics of an MEA, in conjunction with mass and energy balances, to determine the

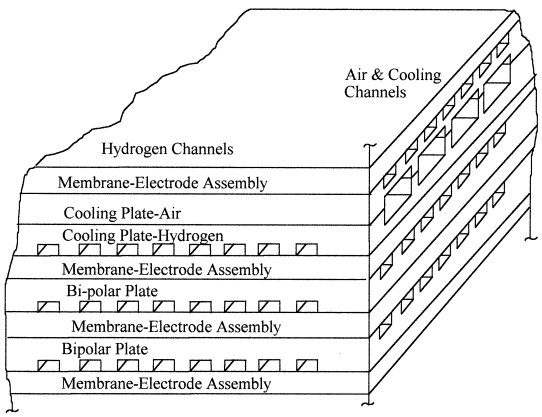

Fig. 1. Schematic diagram of a fuel cell stack [2].

characteristics and performance of a fuel cell stack [3]. This procedure is described in the following sections.

3. Description of the model

A model to be used to investigate the parameters of a fuel cell power system should be able to simulate transient behavior, allow investigation of parameter effects and interactions, and be easily modified to accommodate technical and configuration changes. These aspects of the modeling technique developed for investigating fuel cell system parameters are explained in the following sections.

3.1. Dynamic simulation

To model the transient behavior of a fuel cell stack the modeling technique incorporates an explicit finite difference scheme. This technique requires that the fuel cell stack be divided into elements whose size is determined by the desired accuracy of the results and the numerical stability of the calculations. A schematic diagram of an element (i,j,k), and the surrounding elements that interact with it, is given in Fig. 2. The properties of each element are assumed to be spatially uniform and change with time. Time is measured in discrete steps with the future state of an element calculated using the current state of the surrounding elements, and the material and transport properties of the element. The size of the time steps, like the size of the elements, is determined by the desired accuracy of the results and the numerical stability of the results; the smaller the time step, or element, the greater the accuracy, but the greater the number of calculations that must be completed.

The finite difference scheme is used to calculate the temperature only. The remaining properties are calculated using the temperature and various relationships that will be covered in later sections. As a result, the numerical stability of each calculation is set by the thermal properties of the fuel cell. A numerically stable calculation is one that converges on a solution, whereas an unstable calculation does not.

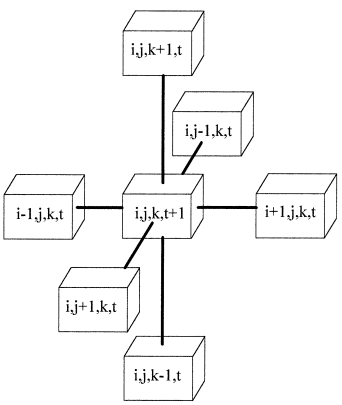

Fig. 2. Schematic diagram of a main element and the surrounding interacting elements (elements are expanded for clarity).

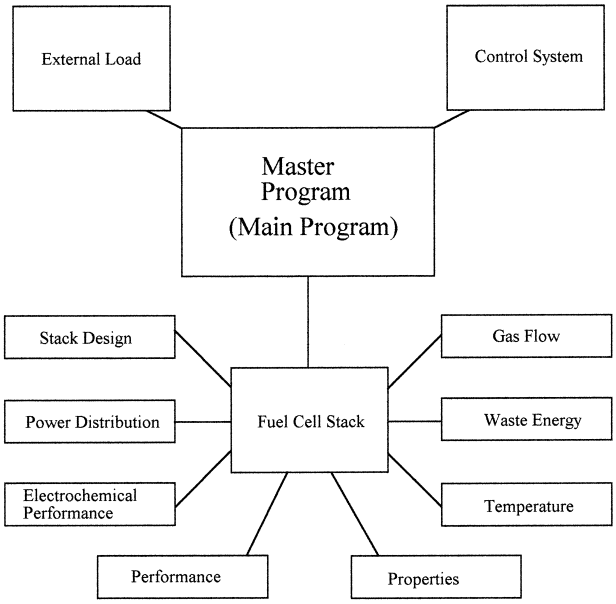

Fig. 3. Diagram of the fuel cell vehicle power system modeling technique.

3.2. Modular design

Separate computational modules are used to model the behavior of each component of the fuel cell power system. All of the modules are independent of each other so components can be changed without rewriting an entire model. This makes a model developed using this technique easy to change, an asset when used for parameter investigations and when modifications to a model are required to account for technical advances in fuel cell systems.

The fuel cell stack system is divided into four modules; the Master program, the External load, the Control system, and the Fuel cell stack. The Fuel cell stack is further subdivided into sub-modules to accommodate the large number of processes and design options associated with a stack. Fig. 3 is a diagram showing each of the modules and their relationship to the overall model. A description of each of the modules and sub-modules follows.

3.2.1. Master control

The master control module controls information flow. When modules need input from other modules, or the user, this information passes through the master control module. No calculations are conducted in the master control module, only information handling is performed.

3.2.2. External load

The external load module specifies the load that the fuel cell stack system must deliver. The load can be varied in

any manner that the user chooses. The load can be in the form of an equation or a look up table.

If the load specified is for a vehicle, the losses associated with the rolling resistance, wind load, mechanisms, etc. should be added to the power required to move the vehicle to obtain the load. Parasite losses associated with the fuel cell system, i.e., compressor losses, electrical resistance, etc., are accounted for in the model and should not be added externally to the load.

3.2.3. Control system

The control system module regulates the entire stack system. It determines the amount of process gas required to meet a particular load as well as calculates the amount of energy used to deliver the gas to the fuel cells. The control module also calculates the amount of cooling flow required by the stack to maintain the desired temperature. If the stack is pressurized the energy required to pressurize the system will be calculated in the control system module.

The amount of process gas required, and the amount of water produced, by the fuel cell stack is calculated using the electrochemical equations that describe the local reactions [3].

$$\text{Anode: } H_2 \Leftrightarrow 2H^+ + 2e^- \quad (1)$$

$$\text{Cathode: } 1/2O_2 + 2H^+ + 2e^- \Leftrightarrow H_2O \quad (2)$$

$$\text{Overall: } H_2 + 1/2O_2 \Leftrightarrow H_2O \quad (3)$$

Eq. (1), and the relationship between number of electrons and current, is used to determine the amount of hydrogen needed to meet the local load. Then Eq. (2) is used to determine the amount of oxygen needed to maintain the reaction, and Eq. (3) is used to determine how much water is produced during the reaction. The control system module calculates the amount of gas required and produced by each element and then sums these amounts to obtain the total flowrate required at the stack inlet and the amount of water that will be present at the outlet. If air is used as the source of oxygen the inlet flowrate is increased ($4.76 \cdot O_2$ flowrate) to account for the nitrogen and other gasses present in the air. The method for determining the local load and current will be covered later in this section and a more detailed description of the electrochemical equations is given by Lee and Lalk [2].

The work done on the gases to move them to the stack and to pressurize them is calculated using a form of the equation of Bernoulli: [4]

$$w_p = \frac{\Delta p}{\rho} + \frac{v_2^2 - v_1^2}{2 g_c} \quad (4)$$

Where w_p is the pump work, Δp is the change in pressure between ambient and the stack inlet, ρ is the local density of the gas, v is the gas velocity at ambient (1) and at the stack inlet (2), and g_c is the acceleration due to gravity. To calculate the actual input work to the pump the work done on the gasses is multiplied by an efficiency to account for losses associated with the pump. The parasite power losses are calculated by multiplying the pump work by the fluid flowrate that was calculated previously by the module.

The maximum and minimum stack temperatures are used to determine the cooling flow required. The control strategy tracks the maximum and minimum temperatures and if they exceed preset limits the cooling flowrate is increased, or decreased, by a standard amount. The frequency at which the cooling flow is adjusted, as well as the size of the adjustment is variable. The power required to deliver the cooling flow is added to the parasite power using the method described above.

There is currently no control strategy prescribed on the control system module. That is, it is assumed that power levels, flowrates, and cooling flows change instantaneously when the controller receives a signal. This is an assumption that could be investigated by introducing realistic component and system response times.

3.2.4. Fuel cell stack

The fuel cell stack module models all of the processes and interactions that occur inside the stack. Due to the large number of operations that must be accounted for, the stack is subdivided into eight sub-modules. These sub-modules include Stack design, Power distribution, Polarization—fuel cell electrochemical performance, Gas flow, Waste energy, Temperature, Performance, and Properties. These are described in the following sections.

3.2.4.1. Stack design. The stack design module defines the physical characteristics of the stack. Items that are defined include the size and shape of the bipolar and end plates, the design of the gas delivery and distribution system, the design of the cooling plates, and the material properties of each physical component of the stack. The module also defines the number of MEAs to be included in the stack as well as the number and location of the cooling plates. Nonphysical components defined in this module include the types of reactant gases, the type of cooling fluid, and the operating pressures. The modeling technique is designed so that these values can be input from the program operator or a specified input file.

The stack design module also calculates the volume and mass of the stack using the component designs, the material properties, and the assembly technique. The calculation of volume and mass include the fuel cell stack only and do not currently include additional system components.

3.2.4.2. Polarization—fuel cell electrochemical performance. The polarization curves of the MEAs, the electrical characteristics of the MEAs, and the stack load are combined in the polarization module to calculate the electrical performance of the stack. The polarization curves represent the voltage–current characteristics of the electrochemical

reaction that occurs in the MEA. A typical polarization curve, cell voltage–cell current plot, is shown in Fig. 4. The performance of the MEA depends on several variables including the type of membrane, structure of the electrodes, oxidant used, and the temperature, pressure and humidity of the reaction site. As a result, multiple curves corresponding to various reaction site conditions, exist for each type of MEA.

An empirical equation, derived using data collected from laboratory scale single cells, is used to model these relationships. The empirical equation used for PEMFC stack models relates the voltage of the element to its current [5]:

$$V_e = V_{eO} - b\log(i) - Ri - me^{ni} \quad (5)$$

Where V_e is the local voltage, V_{eO} is the open circuit voltage, i is the local current density, and b, R, m, and n are empirical constants. The constants in Eq. (5) represent losses that cause a reduction in voltage as a function of current. The constant b is associated with the kinetic losses in the reaction, R is associated with the ohmic losses due to the electrical resistance of the membrane material, and m and n are constants that account for the losses associated with transporting the process gasses to, and removing the water from, the reaction sites. The values of the constants in Eq. (5) vary depending on many variables, including the composition of the MEA, the fuel and oxidant used, and the local temperature, pressure, and humidity of the MEA. Variations in these variables are modeled by changing the values of the constants.

The procedure used to locate the point on the polarization curve, at which each computational element will operate was developed using the electrical characteristics of stack components and the empirical equation of the polarization curve. The material of the electrodes and bipolar plates make them equal potential surfaces. This electrical characteristic means that the potential over the entire surface of an electrode or bipolar plate is the same. Thus, each MEA has one potential at any instant in time. In addition, at any instant in time, each MEA in a stack may have a different potential, and the potential of every MEA will vary with time.

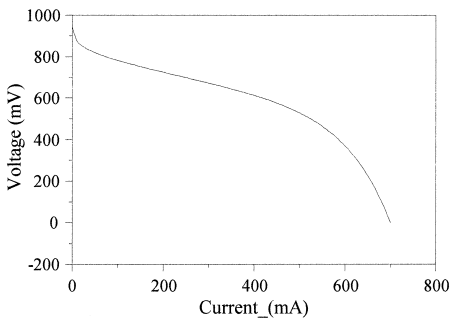

Fig. 4. Voltage variation with current for a typical PEMFC.

Another electrical characteristic used to develop the procedure is that the electrons required for the electrochemical reaction of an MEA are supplied by the anode of the MEA that shares a bipolar plate with the cathode of that MEA. A consequence of this characteristic is that the current produced by each MEA must be the same. The current may be different at various locations on an MEA surface. However, the sum total current through each MEA in the stack must be the same at any instant in time (MEAs are electrically in series).

The procedure for determining the operating point on the polarization curve uses an estimate of the voltage, the empirical equation of the polarization curve, and an iteration routine to calculate the corresponding current. For the initial time step, it is assumed that the stack starts with a constant temperature, pressure, and humidity (usually ambient). Therefore, the same polarization curve represents the performance of every power producing computational element on all MEAs of the stack. The procedure then divides the load by the number of power producing elements to determine an elemental power requirement for each element. Eq. (5), or equivalent empirical equation, and the relationship between voltage and power is then used to obtain an empirical expression for elemental power that can be used with an iteration routine to locate the point on the polarization curve that will produce the required elemental power.

$$P_e = iV_{eO} - ib\log(i) - Ri^2 - ime^{ni} \quad (6)$$

Where P_e is the local power and the other terms are from Eq. (5).

For subsequent time steps the initial value for the MEA voltage is set equal to the previous time step voltage of the corresponding MEA. Once the voltage for each MEA is obtained Eq. (5) is used, along with an iteration routine, to obtain the electrical current values for each MEA. The local temperature, pressure, and humidity are also required to determine the values of the constants in Eq. (5). The values for the voltage and current of each element are then sent to the power distribution module so that the values can be compared to the specified load and current requirements.

If adjustments need to be made to the voltage, to meet the load or the electrical current requirements, the new value of the voltage will be determined in the power distribution module and sent back to the polarization module. The new voltage is then used with Eq. (5) and the iteration routine to calculate the new current. The new values are then sent back to the power distribution module. This process is continued until the load and the electrical requirements are met.

3.2.4.3. Power distribution. The power distribution module determines if the power produced will meet the load and if the sum total current of each MEA is the same. Maintain-

ing a consistent sum total current among MEAs is required by the electrical characteristics of the fuel cell stack. If corrections to the power or current of the elements is needed, the amount of the change is determined in the power distribution module.

The power distribution module initially multiplies the voltage and current of each element and then sums the products to obtain the power produced by the stack. The total power is then compared to the load to ensure that the power produced is not only greater than the load, but also that it is not too large. The difference between the load and the power produced is used to make adjustments to the voltage.

The total current of each MEA is then computed and checked for variation. To accomplish this, the sum total current of each MEA is calculated by summing the current of all power producing elements on a particular MEA. These totals are then sorted from largest to smallest and the greatest variation calculated by subtracting the smallest sum total current from the largest sum total current. The difference in current is then compared to a set variation limit; if the difference is smaller than the standard, and the power is within the acceptable level, the program advances to the next module, otherwise corrections are made to the voltage and the updated values are returned to the polarization module.

Corrections to the power and sum total current produced by an MEA must be made by changing the voltage of the MEA. This is to ensure that the electrical characteristics of the fuel cell stack are maintained. Since the power and current are both affected by changes in voltage, the expression used to determine the new MEA voltage addresses both.

$$V_{e_{NC}} = \frac{NP_{e_{OC}}}{i_{ave} + (N-1)i_{OC}} + \frac{\Delta P_{e_{stack}}}{Ni_{OC}} \tag{7}$$

Where V_{eNC} is the new element voltage, N is the number of cell in the stack, P_{eOC} is the power produced by the element prior to the voltage change, ΔP_e is the required change in power produced by the stack in order to meet the load, i_{ave} is the average current of the stack, and i_{OC} is the current of the element prior to the voltage change.

The new voltages, one for each cell in the stack, are then sent back to the polarization module where corresponding element currents are calculated. This process is continued until the electrical characteristics are satisfied and the power produced is within a prescribed acceptable range. A more detailed description of the procedure used to calculate the electrochemical performance is given in Ref. [2].

3.2.4.4. Gas flow. The gas flow module uses the flowrate information from the control module, the electrochemical equations, and the design of the bipolar plates to determine the flowrates of each of the process and product gasses at each element. This is accomplished by first dividing the total flowrate of each gas, calculated in the control module, by the number of bipolar plates in the stack and again by the number of flow channels in each bipolar plate. This process produces the total mass flowrate of a gas at the channel inlet.

$$\dot{m}_{x_{inlet}} = \frac{\dot{m}_{x_{total}}}{Nn_c} \tag{8}$$

Where $\dot{m}$ is the mass flowrate of gas x, the inlet subscript represents the inlet of a bipolar plate channel, the total subscript represents the flowrate of gas x at the inlet of the stack, N is the number of bipolar plates in the stack, and n_c is the number of flow channels in a bipolar plate.

The local mass flowrate through each element, for each constituent, is calculated using the mass flowrate at the channel inlet, the element current, and the electrochemical equations. The element current and electrochemical equations are used to determine the amount of fuel and oxygen used (the amount of water produced) at the first element after the inlet to the bipolar plate and this amount is subtracted from (added to) the inlet mass flowrate. The mass flowrate for the next element along the bipolar plate flow channel is calculated using the same procedure only the mass flowrate exiting the previous element is substituted for the inlet flowrate. This process is repeated until the end of the flow channel is reached. For example, the equation used to determine the local mass flowrate of air at element (i,j,k) is given by Eq. (9).

$$\dot{m}_{air_{i,j,k}} = \dot{m}_{air_{i-1,j,k}} - 0.0004\, i_{i,j,k} \tag{9}$$

Where $\dot{m}$ is the mass flowrate of air of element i,j,k and the previous element, and i is the current of element i,j,k.

The product water is produced at the cathode so the oxidant (air) and product water share the same channels. Their individual mass flowrates are therefore combined to determine the total mass flowrate in the channels on the cathode side of the bipolar plate. Hydrogen, or hydrogen rich gas if a reformer is used, is the only gas in measurable quantities in the channels on the anode side of the bipolar plate.

3.2.4.5. Waste energy. The waste energy module computes the amount of available energy that is not converted to electrical power due to losses from irreversible processes associated with the electrochemical reaction. The module also computes the amount of electrical energy that is converted to thermal energy as a result of losses inside the stack. The magnitudes of the losses are computed and combined to obtain the total waste energy associated with an element. The total is then sent to the temperature module where it will be used as part of the temperature calculation. The waste energy is the amount of energy that must be removed from the fuel cell stack in order to maintain a constant temperature.

To determine the amount of waste energy in an element originating from the losses in the electrochemical reaction, the difference between the thermodynamic potential of the fuel (hydrogen) and the actual voltage of an element are multiplied by the element current. The derivation of the thermodynamic potential is given in Ref. [2].

$$Q_{P_{i,j,k}} = \left(E_T - V_{ei,j,k}\right) i_{i,j,k} \quad (10)$$

Where Q_P is the energy from the fuel not converted to electricity, E_T is the thermodynamic potential of the fuel, V is the voltage of the element, and i the current of the element.

Electrical losses in an element are due to the electrical resistance (ohmic) of fuel cell stack materials and the resistance that exists when electricity flows between stack components (contact resistance). The calculation of ohmic losses is accomplished by multiplying the electrical resistance of each material in an element by the electrical current passing through the element. The amount of waste energy from electricity flowing between stack components is also determined by multiplying the numerical value of the contact resistance by the element current. Values for contact resistance are obtained experimentally for different interfaces.

3.2.4.6. Temperature. The temperature module computes the temperature distribution throughout the stack. This is accomplished using an energy balance:

$$E_{i,j,k_{in}} - E_{i,j,k_{out}} = \Delta E_{i,j,k_{stored}} \quad (11)$$

Where E is the energy in an element. Energy flows in and out of an element in the form of heat and mass transfer. The change in energy stored results in a change in temperature. The change in temperature of an element is calculated using the mass and thermal capacitance of the element.

$$\Delta E_{i,j,k_{stored}} = m_{i,j,k} C \Delta T \quad (12)$$

Where ΔE is the energy stored in element i,j,k, m is the mass of the element, C is the thermal capacitance of the element, and ΔT is the change in temperature of the element.

3.2.4.7. Performance. The thermodynamic efficiency of the fuel cell is calculated in the performance module. This is accomplished by dividing the net electrical energy produced by the energy value of the fuel used to produce the electricity. The net electrical energy is calculated by numerically integrating the net power with respect to time. The mass of the fuel is obtained by summing the fuel used by each element during each time interval and then summing the fuel used each time step. The modeling technique allows for either the higher or lower heating value of the fuel to be used for this calculation.

$$\eta_{th} = \frac{\int P_e \mathrm{d}t}{HV_{fuel} m_{fuel}} \quad (13)$$

Where η_{th} is the thermodynamic efficiency of the stack, P_e is the net power produced by the stack, HV is the heating value of the fuel, and m is the mass of the fuel used to produce the power.

The thermodynamic efficiency of the stack is the main performance parameter of interest when comparing fuel cells of equivalent power rating. The module calculates the thermodynamic efficiency for each time step and for the entire cycle simulated.

3.2.4.8. Properties. Pressure and humidity profiles are the output from the properties module. These profiles are computed using the design of the bipolar plates, output from the flow module, the ideal gas equation, and psychometric relationships. The bipolar plate design, output from the flow module, and the ideal gas equation are used to calculate the density and velocity of the gases in the flow channels; both of which are required to calculate the pressure drop. Due to the low velocity of the gases in a flow channel, a laminar velocity profile will be assumed when computing the pressure drop [4]. The output from the flow module and the psychometric relationships are used to calculate the humidity [6].

$$\Delta p = \frac{0.316 \rho L v^2}{8 \mathrm{Re}^{25} R_h} \quad (14)$$

$$\phi = \frac{Wp}{(0.622 + W) p_{ws}} \quad (15)$$

Where Δp is the change in pressure between the inlet and outlet of an element, ρ is the density of the gas, L is the length of an element, v is the velocity of the gas, Re is the Reynolds number of the gas, R_h is the hydraulic radius of the bipolar plate channel, ϕ is the relative humidity of the element, W is the humidity ratio of the element, p is the element pressure, and p_{ws} is the water saturation pressure.

4. Implementation

The modeling technique can be implemented using any scientific computer language. FORTRAN is preferred by the authors because of its wide acceptance and homogeneous application but C, C++, or any of the BASIC languages can be used. A model can be developed to run on a personal computer. However, if large fuel cell systems are to be modeled a work station or mainframe computer will be required.

5. Results

The modeling technique described above was specifically designed to aid in investigating the parameters and parameter interactions of a fuel cell power system. The information required for each investigation will vary depending on the parameters being investigated and the effects on the fuel cell stack (dependent variables) of interest. As a result, the modeling technique was designed so that the output from a model can be varied to meet the needs of individual investigations. Results can be in the form of single values, for example the total mass and volume of a stack, or in the form of distributions, i.e., the variation of outlet temperature as a function of time. The remainder of this section will give examples of both types of results.

5.1. Sample results

Samples of the type of results that can be obtained using a model developed using the modeling technique described above are described and listed. The design specifications of the fuel cell stack modeled for the example are listed in Table 2.

The load for the example was a sine wave that closely resembled the power profile required for a mid-sized passenger vehicle to meet the Generic Simplified Urban Driving Schedule (GSFUDS), the cycle often used to compare the performance of electric vehicles [7].

Table 2
Design specifications for the fuel cell stack

Parameter	Description
Operating	
Pressure	5 atm
Temperature	70°C
Humidity	45% at stack entrance
Stoichiometry	Air = 3, hydrogen = 1.2
Design	
Membrane–electrode assembly	
Membrane	Nafionc® 117
Catalyst	Platinum
Electrode	E-TEK®
Stack	
MEA active area	350 cm^2
Aspect ratio	2
Number of cells	125
Bipolar plate material	Low porosity carbon graphite
Flow configuration	Counter flow
Gas delivery strategy	Parallel flow
Cooling plate material	Low porosity carbon graphite
Cooling fluid	Air
Cooling plate frequency	1 cooling plate/2 cells
Stack construction	Bonding
Manifold	External

Table 3
Single value results from the model

Result	Value
Total volume of the stack	41,700 cm^3
Total mass of the stack	34.5 kg
Hydrogen use	135 g/h
Total cycle efficiency	56%

The maximum load of the cycle was 40 kW and the maximum power capability of the example fuel cell stack is 4.8 kW. As a result, it was assumed that a vehicle would carry nine fuel cell stacks in a modular configuration with each fuel cell stack contributing equally to the load. The load and all of the sample results given are for a single module. Eq. (16) represents the load for the example.

$$\text{Load} = 2.5 + 2\,SIN\left(\frac{\pi t}{30}\right) \tag{16}$$

The sample output was computed using two different sizes of computational elements. This was done to check the stability of the model. One simulation used computational elements that were 1 cm^2 and for the other simulation 0.25 cm^2 computational elements were used.

Results from the two simulations were very comparable. The maximum deviation between corresponding results was less than 5%. This difference is attributed to the iteration routine used to calculate the power produced by the fuel cell stack. Therefore, it was concluded that the model was stable using 1 cm^2 computational elements for this fuel cell stack configuration.

5.1.1. Single value results

Table 3 is a list of the significant single value results. These results include the volume and mass of the fuel cell stack, the mass of hydrogen used by the fuel cell to meet the load for 1 h, and the total cycle efficiency. The total cycle efficiency is calculated for the number of complete load cycles run in 1 h.

Single value results are those that are most often used for parameter investigations because they are the main variables of interest when designing a fuel cell power system. These variables indicate the size, mass, and range

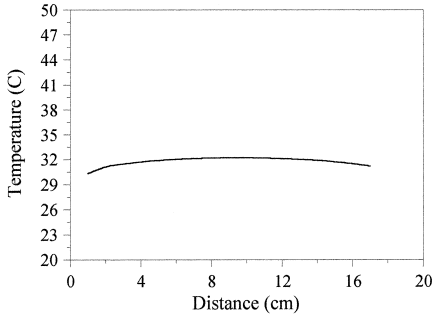

Fig. 5. Fuel cell temperature as a function of distance along the length of a fuel cell stack.

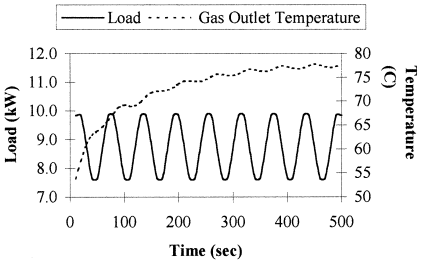

Fig. 6. Average exit temperature of the process air of a fuel cell stack as a function of time.

capability of a vehicle or the construction and operating costs of an electrical generating plant. By understanding how the fuel cell stack parameters affect the single value results, a designer can choose the stack configuration that will best fit an application.

5.1.2. Distribution results

Figs. 5–7 are examples of distribution results. Fig. 5 shows the stack temperature as a function of the distance along the length of the fuel cell. The temperature was calculated at the centerline of the middle MEA.

The variation of the average exit temperature of the air with time is shown in Fig. 6. The load on the fuel cell stack is also shown. It should be noted that the temperature profile lags the load profile by several seconds. This is due to the thermal capacitance of the fuel cell stack.

Fig. 7 shows the thermal efficiency of a fuel cell stack as a function of time. The load on the fuel cell stack is also shown as a reference. The 180 phase shift between the two profiles indicates an increase in performance with decreasing load. This aspect of fuel cell performance is desirable for vehicle applications.

The main function of distribution results is to identify potential problems that could make a particular combination of parameters undesirable. Combinations of parameters that result in fuel cell stacks with excessive cell temperatures, pressure drops, or water accumulations should be avoided because these combinations could result in reduced performance and/or lifetime of the stack.

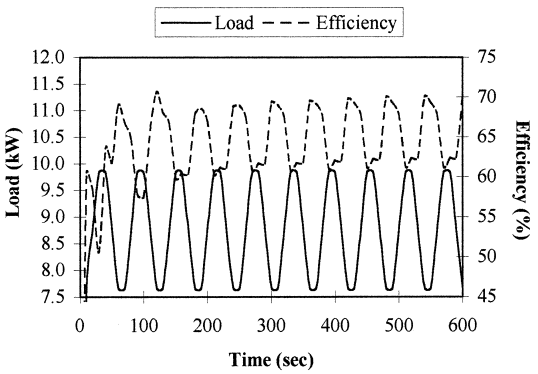

Fig. 7. Thermal efficiency of a fuel cell stack as a function of time.

Many other types of distribution results are possible including the pressure, humidity, and oxygen concentration of the process air, the pressure and temperature of the fuel, and the temperature of stack components, all as a function of both time and position in the fuel cell stack. The results produced by a model can be customized to meet the needs of the investigation being conducted.

6. Verification investigation

In order for the model to be useful as a tool for designing a fuel cell stack, it must be able to accurately simulate the performance of an actual stack. An experimental investigation was conducted to determine the validity of the model. A 50 cm^2 four cell PEMFC stack operating on hydrogen and air at steady state conditions was used for the investigation. The following sections describe the experimental apparatus and procedure. The results from the investigation are presented and discussed.

6.1. Experimental apparatus

The experimental apparatus consisted of a PEMFC stack, the sensors and data acquisition system used to measure and record needed information, and a test stand that provided the electric load, reactant and cooling air flow control, and fuel flow control. Fig. 8 is a schematic diagram of the experimental apparatus.

The PEMFC stack contained four, 50 cm^2 MEAs that were built by the Center for Electrochemical Systems and Hydrogen Research (CESHR) at Texas A&M University. They were constructed using Nafion® 112 membrane material and carbon cloth electrodes (also developed at CESHR). The platinum loading of the anode electrode was 0.4 g/cm^2 and 1.4 g/cm^2 for the cathode. Hydrogen was used as the fuel and air was used as the oxidant.

The bipolar plates used in the stack were constructed of low porosity carbon graphite. They were machined into flat plates 5 mm thick with a serpentine flow configuration

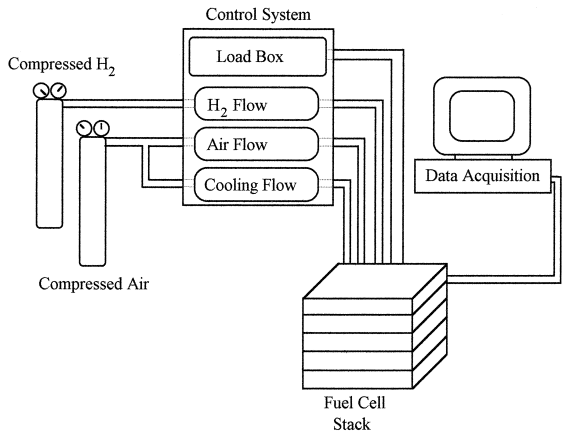

Fig. 8. Schematic diagram of the experimental apparatus used for the model verification investigation.

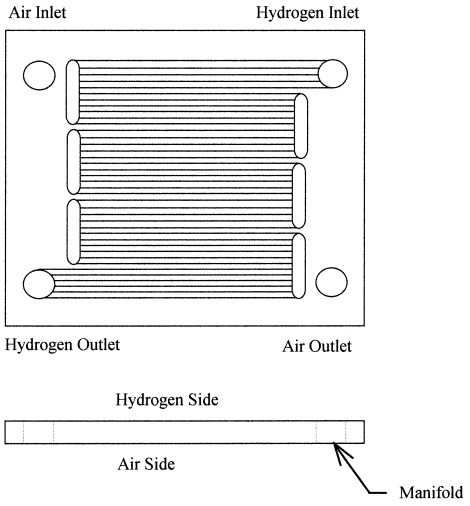

Fig. 9. Schematic diagram of the hydrogen side of the bipolar plates used in the four cell fuel cell stack built for the verification investigation (the details have been excluded for clarity).

cut into each surface. A serpentine flow configuration consists of sets of parallel flow channels arranged in series. The bipolar plates used in the investigation had three parallel channels in a set. The channels were 1 mm^2 and separated by 1 mm (1 mm lands).

The stack had an internal manifold with the reactant gases (hydrogen and air) being delivered in one corner of the plate and removed from the opposite corner. The air and hydrogen sides of the bipolar plate were identical. Fig. 9 is a schematic diagram of the bipolar plates used in the investigation.

One cooling plate set, also made from low porosity carbon graphite, was used to cool the stack. The cooling plate set consisted of two plates that were machined with a flow pattern identical to the bipolar plates on one side and parallel channels on the other. The channels on the cooling side of the plates were the same size as the reactant gas channels (1 mm^2 with 1 mm lands). Each plate in the cooling plate set was 5 mm thick.

The remainder of the stack consisted of the endplates which were made of 2-cm thick copper. Tierods around the perimeter of the end plates were used to hold the stack together. The tierods were tightened with a torque wrench to assure the compressive force that holds the stack together was distributed equally. Table 4 summarizes the stack design and operating conditions used for the verification experiment.

The variables measured included temperatures, pressures, flowrates, inlet air humidity, current, cell potential, and stack voltage. Table 5 lists the data taken at the inlet, in the stack, and at the outlet of the fuel cell. Data taken at the inlet, with the exception of the reactant air and hydrogen flowrates, were used as inputs for the mathematical simulation. Therefore, inlet values, with the exception of the reactant air and hydrogen flowrates, are not given as results.

Table 4
Specifications of the four cell fuel cell stack built for the verification investigation

Parameter	Description
Operating	
Pressure	1 atm
Temperature	50°C
Humidity	100% at stack entrance
Stoichiometry	Air = 3, hydrogen = 1.2
Design	
Membrane–electrode assembly	
Membrane	Nafion® 112
Catalyst	0.4 mg Pt/cm^2 Anode, 1.4 mg Pt/cm^2 Cathode
Electrodes	Carbon cloth prepared by CESHR
Stack	
MEA active area	50 cm^2
Aspect ratio	1
Number of cells	4
Bipolar plate material	Low porous carbon graphite
Flow configuration	Counter flow
Gas delivery strategy	Series–parallel flow
Cooling plate material	Low porous carbon graphite
Cooling fluid	Air (cross flow)
Cooling plate frequency	1 cooling plate/2 cells
Stack construction	Compression bolts
Manifold	Internal

The gas temperatures were measured using thermocouple probes that were placed in the inlet and exit gas streams. The humidity of the reactant air at the inlet was measured with a humidity probe in the inlet gas stream. For the individual cell readings, holes were drilled into the bipolar plates to accommodate temperature and voltage probes. The holes were drilled such that temperatures at the edge of the active area could be monitored. The potential measurement for each cell was taken as the difference between the cell potential and ground, and the total stack potential was taken as the potential difference between the end plates. Finally, the pressure drop across the stack was measured by placing a pressure transducer between the inlet and outlet air delivery tubes. No direct pressure measurements were made.

Table 5
Variables measured for the verification investigation

Inlet	Stack	Outlet
Reactant air pressure	Stack current	Reactant air pressure
Reactant air temperature	Stack voltage	Reactant air temperature
Reactant air humidity	Cell temperature	
Hydrogen temperature	Cell potential	
Reactant air flowrate		
Hydrogen flowrate		
Cooling air flowrate		
Cooling air temperature		

6.2. Experimental procedure

The fuel cell stack described in the previous section was operated at two distinct operating points. The first operating point required the fuel cell to produce a current of 15 A (Run A) and the second operating point required the fuel cell to produce a current of 25 A (Run B). These conditions represented the mid and maximum power production capabilities of the fuel cell stack.

The fuel cell stack was started by applying the 15 amp load (Run A) and adjusting the reactant gas flowrates to the appropriate levels. These levels were calculated using electrochemical equations that describe the reaction and the reactant gas utilization [8]. The cooling air flowrate was set to a value that would allow the desired operating temperature to be achieved. This value had been determined prior to conducting the verification investigation.

The stack was allowed to run for 15 min prior to taking data so that steady state conditions were reached. Data was then taken and recorded once every minute for 5 min. Upon completion of the fifth reading the load and flowrates were changed to the 25 amp load condition (Run B), and the process was repeated. The load conditions were alternated until three runs of each condition were completed.

6.3. Comparison of modeling to experimental results

Data from the verification experiment was analyzed by computing the mean value and standard deviation for each variable measured. A comparison between the mean value and model prediction for each variable is presented in Table 6. The value of the uncertainty included in Table 6 is the larger of the uncertainty of the instrument used to measure the variable, or one standard deviation of the measurements.

As shown in Table 6, the majority of the model predictions of the total stack values for both operating points were within the uncertainty of the variables measured. Of the predictions that deviated from the experimental values, only the total stack voltage and power for Run B (25 A) deviated by more than 5%. The model predictions for both of these variables deviates from the measured value by approximately 15%. The source of both deviations is the same since the power is calculated by multiplying the stack voltage by the stack current.

A potential source of the deviation in stack voltage, and stack power, is the relationship between the uncertainty of the model and the location of the operating point on the power curve. The model uncertainty results from the iteration routine used to determine the potential/current combinations that will produce the desired stack power. The iteration routine adjusts the cell potentials, until the computed value of the stack power is within a prescribed range of the correct value [2]. The range of potentials that will produce an acceptable value for stack power depends on the slope of the power curve; a parabolic shaped plot of the stack power as a function of stack current. To achieve the power requirement of Run B, the fuel cell stack had to operate close to its maximum power output. The power curve for this fuel cell stack has a rounded apex at the maximum power output. The rounded apex indicates that the power is not significantly influenced by the current at the highest power levels. Therefore, the routine may not produce a potential/current combination that is as close to the correct value when simulating operation at maximum power as compared to simulating a lower power output [2].

Table 6
Results of the verification investigation (Run A was a load of 15 A, Run B was a Load of 25 A)

Parameter	Run A		δ [a]	Δ [b]	Run B		δ [a]	Δ [b]	Experimental uncertainties
	Experimental	Model		(%)	Experimental	Model		%	
Stack power (W)	33.48	35.04	1.56	4.7	43.30	36.60	−6.70	−15.4	±1.02
Stack current (A)	14.75	15.30	0.55	3.7	24.60	24.40	−0.20	−0.8	±0.02
Stack voltage (V)	2.27	2.29	0.02	0.9	1.76	1.50	−0.26	−14.8	±0.04
Stack volume (cm^3)	1575	1573	−2	−0.1	1575	1573	−2	−0.1	±3
Stack mass (g)	7200	7200	0	0	7200	7200	0	0	±100
Process air flowrate (SLM)	3.1	3.1	0	0	5.1	5.0	−0.1	−2.0	±0.1
Hydrogen flowrate (sccm)	590	580	−10	−1.7	1010	1030	20	2.0	±20
Stack pressure drop (psi)	2.7	2.8	0.1	3.7	4.4	4.4	0	0	±0.3
Outlet air temperature (°C)	60	59	−1	−1.7	66	68	−23.0	±2	
Temperature of cell 1 (°C)	60	52	−8	−13.3	69	64	−4	−5.8	±2
Temperature of cell 2 (°C)	59	56	−3	−5.1	67	70	−2	3.0	±2
Temperature of cell 3 (°C)	59	53	−6	−10.2	67	64	−3	−4.5	±2
Temperature of cell 4 (°C)	59	52	−7	−11.9	66	62	−4	−6.1	±2
Potential of cell 1 (V)	0.6	0	0	0.5	0.4	−0.1	−20.0	±0.2	
Potential of cell 2 (V)	0.7	0.6	−0.1	−14.3	0.6	0.4	−0.2	−33.3	±0.2
Potential of cell 3 (V)	0.7	0.6	−0.1	−14.3	0.6	0.4	−0.2	−33.3	±0.2
Potential of cell 4 (V)	0.7	0.6	−0.1	−14.3	0.6	0.4	−0.2	−33.3	±0.2

[a] δ = Model value − experimental value.
[b] Δ = (Model value − experimental value)/(experimental value) × 100

The current is not as affected by the deviation between the calculated and actual operating point because of the series configuration of fuel cell stacks. The potential of each MEA in a stack is added together to obtain the total stack output voltage, whereas the stack current is the same for each MEA. As a result, errors in calculated MEA potential are added together to obtain the total stack output voltage error where as the errors in the calculated MEA current are averaged to obtain the total output current error.

Model predictions of individual cell values were not as close to the experimental values as the total stack predictions. Differences between the predicted and measured cell temperatures were as high as 13% and predictions for the potentials of the individual cells varied by as much as 33%. However, the differences between the model predictions and experimental measurements for the cell potentials were all within the uncertainty of the measurements. The large uncertainties were due to the standard deviations of the experimental values.

One reason for these large deviations is that the mathematical model assumes that all of the cells are identical and capable of performing equally, whereas the cells of the actual fuel cell stack vary. These variations caused the performance to vary from cell to cell, and the performance of each cell to vary between replications of the same run. The large standard deviations (and corresponding large uncertainties) of the cell values resulted from the variations.

Possible sources of the cell performance variations include differences in reactant gas flowrates, varying rates of water accumulation, differences in MEAs, and differences in contact resistance between cells. One benefit of the model is that it can be used to identify causes of performance variation, and investigate the relative importance of each cause.

Further analysis of the results presented in Table 6 indicates that the model predicts the trends associated with changes in external load. A comparison of the trends predicted by the model to the trends associated with the experimental results showed that the model predictions matched the experimental results. The trends matched without making any changes to the model except for the external load; it was changed to match the load of each experimental operating condition.

7. Conclusions

The following conclusions were drawn from this investigation: (A) mathematical models created using the modeling methodology, develop by the authors, would correctly predict fuel cell stack behavior. (B) Although models developed using this technique would not be useful for examining the microscopic electrochemistry of the stack, they will be useful to the design engineer that is interested in optimizing system performance given a specified MEA. (C) Considering the results of the verification experiment, the model may be useful in the following applications: (1) investigate the design and operating parameters, and parameter interactions, of a fuel cell system and determine their order of importance; (2) investigate extreme operating conditions in order to conduct a failure modes and effects analysis; (3) conduct a sensitivity analysis of the important design and operating parameters of a fuel cell system; (4) building a simplified model using the results of the sensitivity analysis; (5) estimate the performance of a specific fuel cell system; (6) estimate the performance of a specific application using a specific fuel cell system, for example a passenger vehicle; (7) estimate the effectiveness of proposed solutions to fuel cell system problems, for example proposed solutions for overheating; (8) investigate the effect of alternative fuels and/or oxidizers, for example reformed fuels and oxygen enrichment, on fuel cell system performance.

8. List of symbols

b	Empirical equation constant (mV/dB)
C	Thermal capacitance (J/kg K)
E	Energy of an element (J)
E_T	Thermodynamic potential of fuel (mV)
g_c	Acceleration due to gravity (m/s^2)
HV	Heating value of a fuel (kJ/kg)
i	Current (mA)
L	Length of channel in an element (cm)
Load	Load on fuel cell module (kW)
m	Empirical equation constant (mV)
m_x	Mass of constituent x (g)
$\dot{m}_x$	Mass flowrate of constituent x (g/s)
N	Number of bipolar plate (cells) in a fuel cell stack (dimensionless)
n	Empirical equation constant (cm/mA)
n_c	Number of flow channels in a bipolar plate (dimensionless)
P_e	Electrical power (kW)
p	Pressure (kPa)
p_{ws}	Saturation pressure of water (kPa)
Q_p	Energy from fuel not converted to electricity (J/s)
R	Empirical equation constant (Ω cm^2)
Re	Reynolds number (dimensionless)
R_h	Hydraulic radius (cm)
R_{th}	Thermal resistance of an element (J/K)
T	Temperature (°C)
t	Time (s)
V_e	Voltage (mV)
V_{e_O}	Open circuit voltage (mV)
v	Velocity (cm/s)
W	Humidity ratio of air (dimensionless)
w_p	Pump work (J)

Greek Symbols

ϕ	Relative humidity of process air
η_{th}	Thermal efficiency of the fuel cell stack (%)
ρ	Density (s/cm)

Subscripts

ave	Average value
i,j,k	Element position indices
inlet	Value for the inlet to the element
NC	New voltage or current of an element
stack	Total value for the stack
total	Flowrate at stack inlet
x	Variable constituent

Acknowledgements

The authors would like to thank the National Highway Institute of the Federal Highway Administration for their financial support of this research. In addition, the authors would like to thank the Center for Electrochemical Systems and Hydrogen Research (CESHR) at Texas A&M University for their assistance with the experimental apparatus.

References

[1] J.H. Lee, T.R Lalk, Proceedings, 3rd Annual World Car Conference, University of California, Riverside, CA, 1996.
[2] J.H. Lee, T.R. Lalk, J. Power Sources 69 (1) (1997) .
[3] J.H. Lee, D.H. Swan, T.R. Lalk, SAE Technical Paper Series, No. 931815, Society of Automotive Engineers, 1993.
[4] J.W. Daily, D.R.F. Harleman, Fluid Dynamics, Addison-Wesley, Reading, MA, 1966, pp. 270–275, 322–327.
[5] J. Kim, S. Supramaniam, C.E. Chamberlin, J. Electrochem. Soc. 142 (8) (1995) 2670.
[6] ASHRAE Handbook, 1989 Fundamentals, American Society of Heating, Refrigerating, and Air Conditioning Engineers, Atlanta, GA.
[7] G.H. Cole, SAE Technical Paper Series, No. 891664, Society of Automotive Engineers, 1989.
[8] J.H. Lee, A Methodology for the Development of Mathematical Models for Simulation and Design of Fuel Cell Stacks, Ph.D. Dissertation, Texas A&M University, College Station, TX, 1996.